

Two-dimensional array of coupled nanomechanical resonators

Maxim K. Zalalutdinov^{a)}

SFA Inc., Crofton, Maryland 21114

Jeffrey W. Baldwin and Martin H. Marcus

Naval Research Laboratory, Washington, DC 20375

Robert B. Reichenbach and Jeevak M. Parpia

Cornell University, Ithaca, New York 14853

Brian H. Houston

Naval Research Laboratory, Washington, DC 20375

(Received 15 November 2005; accepted 12 February 2006; published online 3 April 2006)

Two-dimensional arrays of coupled nanomechanical plate-type resonators were fabricated in single crystal silicon using e-beam lithography. Collective modes were studied using a double laser setup with independent positioning of the point laser drive and interferometric motion detector. The formation of a wide acoustic band has been demonstrated. Localization due to disorder (mistune) was identified as a parameter that limits the propagation of the elastic waves. We show that all 400 resonators in our 20×20 array participate in the extended modes and estimate group velocity and density of states. Applications utilizing the resonator arrays for radio frequency signal processing are discussed. © 2006 American Institute of Physics. [DOI: 10.1063/1.2190448]

The collective behavior of coupled nanoelectromechanical system (NEMS) resonators can largely enhance performance of resonator-based devices [radio frequency (RF) filters,¹ added mass sensors,² magnetometers,³ etc.] while preserving the most attractive features of microelectromechanical resonators—superior quality factor, microminiature size, and compatibility with complementary metal-oxide semiconductor (CMOS) processes. When the size of the array exceeds hundreds or thousands of resonators, new capabilities can emerge that are unavailable from a single NEMS device. A coupling between neighboring resonators creates an artificial crystal—a manmade analog of a crystal lattice described in solid state physics in terms of the tight binding approximation.⁴ An acoustic band, formed by splitting individual resonant modes, opens the opportunity for operating with broadband excitations implemented as elastic waves propagating through the array. The theoretical language developed for closely related electromagnetic systems: coupled microwave cavities,⁵ traveling wave amplifiers,⁶ and optical slow wave structures⁷ (SWS), can be largely adopted to describe the elastic waves in mechanical resonators arrays. A rich behavior with a collection of phenomena ranging from intrinsic localized modes⁸ (ILM) to solitons⁹ can be exhibited by such systems.

In practice, however, fabrication of these arrays appears to be challenging due to micromachining tolerances that cause random mistuning of individual NEMS resonators. For larger structures ($270 \mu\text{m}$ long clamped-clamped beams, $f_{\text{res}}=179 \text{ kHz}$) the frequency spread can be confined within 0.8% and existence of collective modes was reported for a linear array of 67 of such resonators.¹⁰ However, the problem becomes more severe when the scaled down devices have nanometer dimensions and exhibit RF frequencies. Excessive mistuning (referred to as a disorder) leads to localization of the acoustic excitations in the array in a way similar to

Anderson's localization¹¹ (AL) and raises the question whether extended modes can be realized in large arrays of coupled nanomechanical resonators.

In order to suppress the localizing effects caused by the disorder we expanded the dimensionality of the arrays from linear to two dimensional. According to AL theoretical models, in two-dimensional (2D) structures the elastic waves are still expected to be localized for an infinitesimal amount of disorder;¹² however, the localization length, λ , can be extended by orders of magnitude compared to one-dimensional (1D) case.^{13,14} In this letter we present our results on the fabrication and experimental study of collective elastic excitations in 2D arrays of coupled plate-type nanomechanical resonators. Each resonator in the array is comprised of a silicon square plate ($2 \times 2 \mu\text{m}^2$ area, 45 nm thickness) supported by a square SiO_2 pillar at the center. The coupling between neighbors is provided by narrow beams (200 nm wide, 45 nm thick) connecting the centers of the square sides (Fig. 1). Commercially available silicon on insulator (SOI) wafers [Si layer, 45 nm; buried oxide (BOX), 150 nm] were used in fabrication. The geometry of the arrays was defined by e-beam exposure of hydrogen silsesquioxane (HSQ) resist

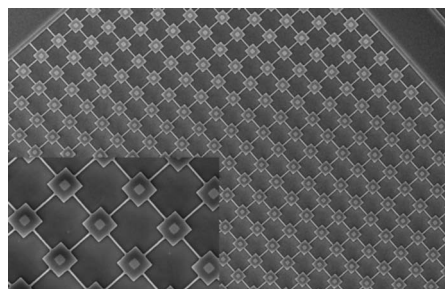


FIG. 1. SEM image showing a section of the paddle resonator array. The size of the silicon square paddles is $2 \times 2 \mu\text{m}^2$, with a thickness of 45 nm. The SiO_2 pillar supporting the center of the paddle has a cross section $0.65 \times 0.65 \mu\text{m}^2$ and is 150 nm tall. The connecting bars are $2 \mu\text{m}$ long and 200 nm wide.

^{a)}Electronic mail: maxim.zalalutdinov@nrl.navy.mil

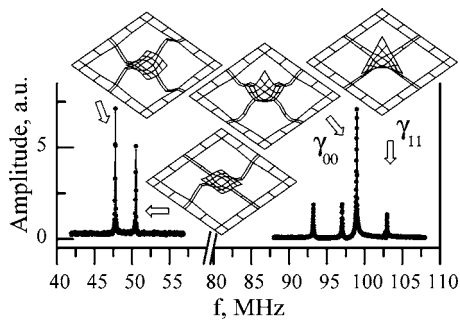


FIG. 2. A vibration spectrum and mode shapes for a single paddle resonator (size identical to that shown in Fig. 1) with connecting arms coupled to a frame.

(Dow Corning FOX-12; thickness, 100 nm)¹⁵ spun on the top of the SOI layer. After developing the resist, a dry etch in a mixed C₄F₈ and SF₆ plasma with the FOX-12 layer as a mask was used to transfer the pattern onto the Si layer. A subsequent wet etch in concentrated HF (48%) removes the rest of the HSQ and partially undercuts the BOX layer releasing the periphery of the Si square plates. The wet etch is timed in order to leave a SiO₂ supporting pillar at the center of the resonator.

To study the vibratory response of the array, we use an optical setup similar to one described elsewhere.¹⁶ A point-type excitation is provided by modulation of the intensity of the blue diode laser (wavelength, 412 nm) focused on a single paddle resonator within the array. The resulting motion can be detected by focusing another laser (red cw HeNe, 633 nm) at any point of the array and measuring the modulation of the intensity of the reflected light. This modulation is provided by a Fabry-Pérot interferometer formed by the paddle itself (acting as a moving semitransparent mirror) and silicon substrate underneath.¹⁷ Low absorption in the very thin (45 nm) Si layer allows us to increase the laser power up to 5 mW without damaging the nanostructures. Independent positioning of the blue (drive) and red (detect) lasers provides the flexibility that is necessary to study the propagation of the elastic waves through the array.

Figure 2 shows the resonant spectrum of an isolated single unit of the array—a test structure comprised of a paddle resonator with 2 μm-long connecting arms bound to an undercut frame. Following the results of finite element analysis (FEA), we denote low frequency peaks (45–55 MHz) as bridge-type vibrations of coupling arms. A high frequency group of resonances (80–100 MHz range) originates from the out-of-plane motion of the paddle itself and includes γ_{00} and γ_{11} modes.¹⁸ All the peaks show a quality factor $Q \sim 3000$ in vacuum $\sim 10^{-7}$ Torr.

A drastic transformation of the vibration spectrum is observed when the paddle resonators are coupled in a square array. The inset in Fig. 3 shows that in a 20×20 array (2×2 μm² paddles, 2 μm long connecting arms, 0.67 μm undercut) the individual levels of the resonators split and create a 27 MHz wide band (91–118 MHz) exhibiting hundreds of sharp peaks. This spectrum was acquired with the blue laser providing excitation at the center of the array and the red laser focused on a resonator 20 μm (five cells) away from the driving point.

In order to study the propagation range of the acoustic waves over our array, spectra similar to that shown in the inset to Fig. 3 were acquired at various distances from the

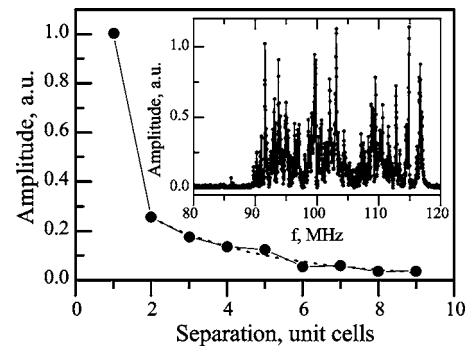


FIG. 3. The inset shows an acoustic band in the vibration spectrum of the 20×20 array of coupled resonators. The excitation was provided at the center of the array and the detection laser was positioned 5 unit cells away. Solid circles in the main plot demonstrate spatial decay of the average acoustic energy of vibrations as a function of separation distance between the drive and detect laser spots. The dotted line shows an exponential fit for the decay.

driving point (excitation was always provided at the center of the array). The solid line in Fig. 3 shows the spatial decay of the band-averaged acoustic energy E_a , calculated as a squared amplitude of the motion of a particular resonator (separated by distance R from the driving point) integrated over 91–118 MHz frequency band. The exponential decay of $E_a(R)$ provides a crude estimate of $\lambda \sim 32$ μm (eight lattice sites) for the localization length calculated according to Ref. 12,

$$\frac{2}{\lambda} = - \lim_{|r-r'| \rightarrow \infty} \frac{\ln t(r, r'; E)}{|r - r'|},$$

where $t(r, r'; E)$ is the energy transmission probability. The high quality factor of our MEMS resonators allows us to rule out dissipation as the factor that limits propagation of acoustic waves in array.¹⁹ We attribute the spatial decay of amplitude to disorder-driven localization, determined by constructive/destructive interference of the acoustic waves that follow different paths along the 2D array. A theoretical value for the localization length λ can be deduced from the known value of the W/V parameter.^{11,20} We estimate the disorder W as a doubled standard deviation (averaged over different modes) of the frequency spread $\sigma_{\text{std}} = 3.6$ MHz exhibited by our test structures (single resonators). The coupling parameter V was extracted from the width of the γ_{11} band ($\Delta f_{11} = 4$ MHz as a result of FEA calculations). The resulting value $W/V = 7$ provides an estimated $\lambda_{\text{theor}} \sim 18$ unit cells according to the results of numerical simulations for 2D disordered media.¹⁴ We find our experimental λ value to be in reasonable agreement with λ_{theor} , considering the limited size of our microfabricated arrays and fact that we have used bandwidth Δf_{11} estimated for one particular mode, while our acoustic band is generated by at least three overlapping modes shown in the high frequency group in Fig. 2.

Stronger coupling and increased density of states for the collective modes of the array can enhance the propagation range. In our 2D arrays, we can implement both approaches by tailoring the geometry of the array. Shortening the connecting arms provides obvious enhancement of the coupling strength between plate-type resonators. Shrinking the central SiO₂ pillar supporting the square resonators (by prolonging HF wet etch time) reduces frequencies for the plate-type vibrations. By combining the effects of shortening the arms

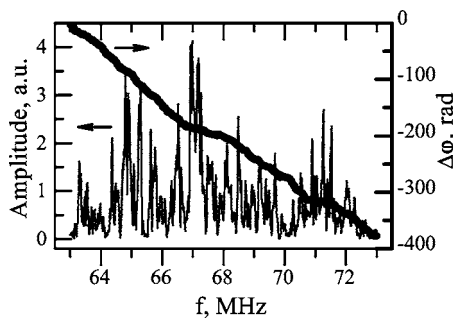


FIG. 4. Enlarged portion of the vibration spectrum and phase shift plot for 20×20 paddle array with stronger coupling (paddle size, $2 \times 2 \mu\text{m}^2$; connecting arms, $1 \mu\text{m}$) and wider undercut (SiO_2 pillar, $0.54 \times 0.54 \mu\text{m}^2$). The spectrum was acquired with a separation of $40 \mu\text{m}$ between drive and detection points. The slope of the $\Delta\phi(\omega)$ line corresponds to a group velocity $V_{\text{gr}} \sim 10 \text{ m/s}$.

and enhancing the plates' undercut, one can shift the frequencies of the bridge-type modes for the connecting arms (45 MHz cluster on Fig. 2) up to the limit where they start overlapping with the plate-type modes of the paddles, thus increasing the density of states. A rectangular 20×20 array with $1 \mu\text{m}$ long arms, $2 \times 2 \mu\text{m}^2$ paddles, and $0.73 \mu\text{m}$ undercut was fabricated according to this recipe. We have found that the spatial decay in the amplitude of the vibration over the entire 20×20 array was only of the order of 50%, i.e., all 400 resonators appear to be involved in the collective motion.

By counting resonance peaks in the vibration spectrum of this array (part of the spectrum is shown in Fig. 4), one can estimate density of states as 13 peaks per MHz (to be compared with $\sim 30 \text{ MHz}^{-1}$ deduced from FEA calculations). The unwrapped phase dependence shown in Fig. 4 provides a mean value for group delay,

$$\tau_{\text{delay}} = \partial\phi/\partial\omega \approx 5.8 \mu\text{s}.$$

From the dimension of the array, $L=60 \mu\text{m}$ one can estimate group velocity, $V_{\text{gr}} \sim 10 \text{ m/s}$. Pronounced kinks in the $\Delta\phi(\omega)$ graph at 67 and 71 MHz illustrate that the group velocity can have a strong frequency dependence. In general, chromatic aberration can alter the group velocity by orders of magnitude in arrays of coupled resonators²¹ and may be exploited for RF signal processing. By converting RF pulses into elastic waves propagating through an inhomogeneous dispersive array, one may be able to implement for example, a broadband spectrum analyzer mimicking Newton's optical prism. More elaborate methods might exploit both normal and anomalous dispersions and effects based on nonlinearity (wave mixing, soliton formation, etc.).

As the next step, we are planning to study diffusivity and dispersion in our structures by fabricating larger arrays and measuring, in the time domain, propagation of short wave packets. Currently we are also taking measures to further refine the fabrication process and reduce the disorder.

To conclude we have fabricated and tested 2D arrays of coupled nanomechanical resonators and demonstrated the

existence of extended modes. Localization of the elastic waves due to fabrication-induced disorder is a key technical challenge but it can be addressed by tailoring the array design. We demonstrate that all 400 resonators in our array were involved in the acoustic band formation and give an estimate of 13 MHz^{-1} for the density of states. We anticipate that NEMS arrays may ultimately have a wide range of applications in sensing and RF signal processing.

The authors gratefully acknowledge Dr. J. Vignola and Dr. D. M. Photiadis for helpful discussions. The authors would also like to thank the members of technical staff of the Institute for Nanoscience at NRL, D. R. King and T. A. Nelson, for help with microfabrication. This work was supported by the Office of Naval Research and Cornell Center for Material Research (CCMR, NSF IDMR-0079992).

- ¹M. U. Demirci, M. A. Abdelmoneum, and C. T.-C. Nguyen, Digest of Technical Papers, The 12th International Conference on Solid-State Sensors and Actuators (Transducers'03), Boston, MA, 8–12 June 2003 (unpublished), pp. 955–958; S. A. Bhawe, D. Gao, R. Maboudian, and R. T. Howe, 18th IRRR International Conference on Micro Electro Mechanical Systems (MEMS 2005), Miami, FL, January 2005 (unpublished), pp. 223.
- ²B. Ilic, H. G. Craighead, S. Krylov, W. Senarathe, C. Ober, and P. Neuzil, *J. Appl. Phys.* **95**, 3694 (2004); K. L. Ekinci, X. M. H. Huang, and M. L. Roukes, *Appl. Phys. Lett.* **84**, 4469 (2004).
- ³D. K. Wickenden, J. L. Champion, R. Osiander, R. B. Givens, J. L. Lamb, J. A. Miragliotta, D. A. Oursler, and T. J. Kistenmacher, *Acta Astronaut.* **52**, 421 (2003).
- ⁴N. W. Ashcroft and N. D. Mermin, *Solid State Physics* (Harcourt Brace, Forth Worth, 1976), p. 176.
- ⁵C. Dembowsky, H.-D. Graf, R. Hoffebert, H. Rehfeld, A. Richter, and T. Weiland, *Phys. Rev. E* **60**, 3942 (1999).
- ⁶J. R. Pierce, *Traveling-Wave Tubes* (Van Nostrand, Princeton, 1950).
- ⁷A. Yariv, Y. Xu, R. K. Lee, and Alex Scherer, *Opt. Lett.* **24**, 711 (1999); H. Altug and J. Vuckovic, *Appl. Phys. Lett.* **86**, 111102 (2005); A. Melloni, F. Morichetti, and M. Martinelli, *Opt. Photonics News* **14**, 44 (2003).
- ⁸M. Sato, B. E. Hubbard, A. J. Sievers, B. Ilic, D. A. Czaplewski, and H. G. Craighead, *Phys. Rev. Lett.* **90**, 044102 (2003).
- ⁹J. W. Feischer, M. Segev, N. Efremidis, and D. N. Christodoulides, *Nature (London)* **422**, 147 (2003).
- ¹⁰E. Buks and M. Roukes, *JMEMS* **11**, 802 (2002); R. Lifshitz and M. C. Cross, *Phys. Rev. B* **67**, 134302 (2003).
- ¹¹P. W. Anderson, *Phys. Rev. A* **109**, 1494 (1958); R. L. Weaver, *Phys. Rev. B* **49**, 5881 (1994); D. M. Photiadis and B. H. Houston, *J. Acoust. Soc. Am.* **106**, 1377 (1999).
- ¹²B. Kramer and A. MacKinnon, *Rep. Prog. Phys.* **56**, 1469 (1993).
- ¹³J. Judge, B. Houston, D. M. Photiadis, and P. C. Herdic, *J. Sound Vib.* **290**, 1119 (2006).
- ¹⁴A. MacKinnon and B. Kramer, *Z. Phys. B: Condens. Matter* **53**, 1 (1983).
- ¹⁵D. P. Mancini, A. Gehoski, E. Ainley, K. Nordquist, D. J. Resnik, T. C. Bailey, S. V. Sreenivasan, J. G. Ekerdt, and C. G. Willson, *J. Vac. Sci. Technol. B* **20**, 2896 (2002).
- ¹⁶M. Zalalutdinov, K. L. Aubin, C. Reichenbach, A. T. Zehnder, B. H. Houston, J. M. Parpia, and H. G. Craighead, *Proc. SPIE* **5116**, 229 (2003).
- ¹⁷D. W. Carr and H. G. Craighead, *J. Vac. Sci. Technol. B* **15**, 2760 (1997).
- ¹⁸P. M. Morse and K. U. Ingard, *Theoretical Acoustics* (Princeton University Press, Princeton, 1968) p. 213.
- ¹⁹M. P. Castanier and C. Pierre, *J. Sound Vib.* **168**, 479 (1993).
- ²⁰D. Thouless, *Ill-Condensed Matter*, edited by R. Balian, R. Maynard, and G. Toulouse (North-Holland, Amsterdam, 1979) p. 5.
- ²¹A. Melloni and F. Morichetti, *Opt. Quantum Electron.* **35**, 365 (2003); W. J. Kim, W. Kuang, and J. D. O'Brien, *Opt. Express* **11**, 3431 (2003).